A 12-mW 264-MHz high linearity sharp roll-off CMOS opamp-RC low-pass filter for MB-OFDM UWB systems

Anh Tuan Phan · Ronan Farrell · Sang-Gug Lee

Abstract This paper presents a high linearity wideband sharp roll-off Opamp-RC low-pass filter (LPF) for Ultra wideband (UWB) applications. The proposed LPF is composed of three biquads' transfer functions with different Q-factors in series. Sharp roll-off is attributed to the steep slope of the peaking of a biquad transfer function with a high Q-factor. The superposition of these biquads also helps extend the bandwidth of the overall LPF transfer function without the cost of extra power dissipation. The effects of biquad arrangements on noise and linearity performances are investigated. A simple operational amplifier (op-amp) is adopted to ensure high frequency characteristics and high linearity performance for the designed filter. The LPF is implemented in 0.13-μm IBM CMOS process from 1.5 V supply. The measured cutoff frequency is 264 MHz with the pass-band ripple of less than 1 dB. Digital frequency tuning is implemented with 40% of tuning range around the cutoff frequency. The amount of out-of-band rejection at 290 MHz and at twice cutoff frequency is 12 dB and about 50 dB, respectively. Good linearity with IIP3 of 23 dBm is obtained. The 6th-order LPF dissipates only 12 mW with the active chip size of $400 \times 640 \ \mu m^2$.

Keywords High frequency filters · Op-amp · UWB · LPF · Sharp rejection · CMOS

A. T. Phan (✉) · R. Farrell
Institute of Microelectronics and Wireless Systemsm, Electronic Engineering Department, National University of Ireland, Maynooth, Maynooth, Kildare, Ireland
e-mail: aphan@eeng.nuim.ie

S.-G. Lee
Information and Communications University, Daejeon, South Korea

1 Introduction

Ultra wideband (UWB) systems for wireless personal area network (WPAN) has recently emerged and drawn great attractions and concerns from the market as well as researchers. With frequency range from 3.1 to 10.6 GHz [1], UWB system can be categorized into two approaches, single band (impulse radio) and multiple bands. For the multi-band approach, multi-band orthogonal frequency division multiplex (MB-OFDM) UWB [2], the spectrum is divided into several sub-bands of 528 MHz. Thus, MB-OFDM UWB can be implemented with very high data rate up to 480 Mb/s to meet the increasing demands of consumers for fast data transmission.

Low-pass filter (LPF) is a key building block in the transmission system, mostly designed for channel selection and anti-alias. In MB-OFDM UWB [3], 7.5 GHz spectrum is divided into 14 bands of 528 MHz as shown in Fig. 1(a), each of these channels can easily cause the interferences on adjacent ones and vice versus. Therefore, the accumulated interferences from other channels can overlap on one given channel. Because of that severe inherent characteristic of MB-OFDM UWB, high performance LPF for channel selection is needed.

Recently published works on LPF for UWB show high frequency characteristics, however, the rejection ratio is moderate with large power consumption [4–6]. For wideband LPF design, G_m-C LPF is often used but it is limited in linearity, dynamic range and sensitive to parasitic [7]. These limitations can be overcome with active-RC LPF approach. However, previously reported works of active-RC LPF are often for narrow band applications and most papers show the cutoff frequency in the range of a hundred MHz are G_m-C type [8–12]. It is due to the open-loop structure and excellent gain-bandwidth property of G_m-C

Fig. 1 a Channel planning for UWB spectrum and **b** UWB channel selection requirement for UWB LPF
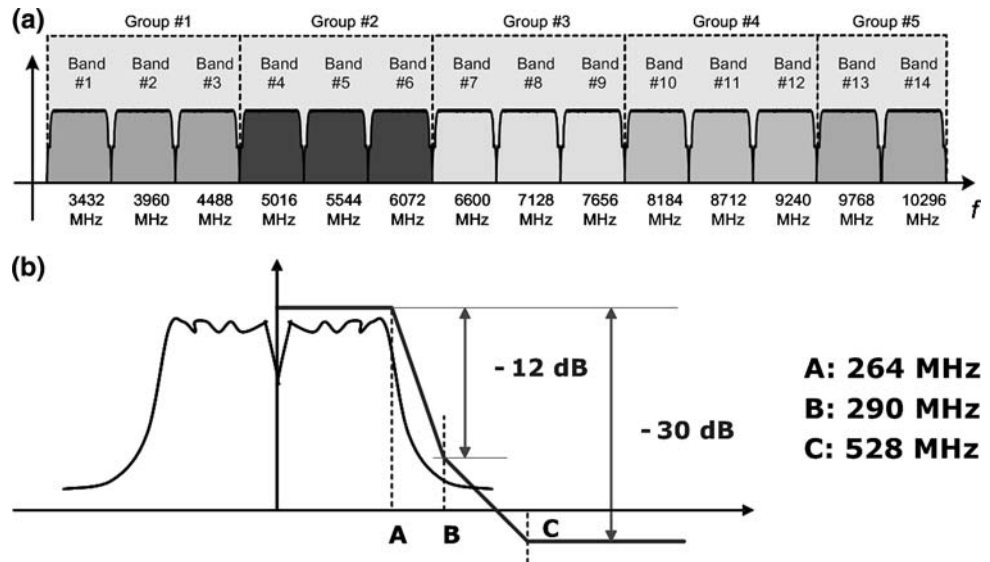
integrator. In wideband active-RC LPF, high loop gain at high frequencies requires high gain bandwidth product. Thus, the trade-off between high frequency characteristic and the cost of high power consumption always poses a challenge for designers.

In this paper, a wideband, high linearity operational amplifier (op-amp) RC LPF for UWB with sharp stop-band characteristic is presented. A special technique to increase the roll-off and extend the bandwidth of the filter is proposed without cost of power dissipation. A simple op-amp is adopted to ensure high frequency performance of the designed filter with low current consumption. Digital tuning is implemented to deal with process variation. The filter is designed in 0.13-μm CMOS process. The proposed filter, compared to other early designs of wide band op-amp RC LPF, shows very good performance, proving itself suitable for wideband applications like UWB.

The remaining paper is organized as follows. Section 2 presents the filter configuration consideration. The sharp roll-off technique is proposed in Sect. 3 with discussions and considerations for the structural effects on NF and linearity performance. The detail LPF design is presented in Sect. 4. Section 5 presents the measurement results. Finally, Sect. 6 concludes.

2 Filter system considerations

The direct conversion receiver architecture shows a great potential to achieve highest integration level of wireless transceiver with low power consumption. In this approach, LPF is critical block to filter out undesired channels and interferences. Each MB-OFDM UWB channel is 528 MHz wide thus the required cutoff frequency (f_c) of LPF is 264 MHz. As aforementioned, the LPF is required to have very high out-of-band rejection ratio due to dense channel spacing in frequency plan, shown in Fig. 1(a). The required rejection is the difference between the received interferer power, the wanted UWB power level, and the SIR. The filtering specification can be calculated from the required sensitivity (80.5 dBm for 110-Mb/s mode), the assumed interferer scenario, and the required receiver signal-to-interferer ratio (SIR) of 6 dB at the output of the filter [13].

In this design, the frequency of concern for 12 dBr rejection is at 290 MHz which is the most challenging, and 30 dBr at twice the cutoff frequency of 528 MHz, shown in Fig. 1(b).

High linearity feature is also demanded, hence, out of band interferences do not create inter-modulations which fall in the pass-band. From the system performance analysis, the allowed in-band ripple is 1 dB and the required group delay is 6 ns, which is based on the ADC performance design [3].

The order of the filter is determined based on the type of filter, cutoff frequency and signal rejection ratio requirement. Classical configurations are Bessel, Chebysheve, Elliptical and Butterworth filters. Among them, Butterwoth gives a high rejection ratio with the same order while requires a reasonable Q-factor. Butterworth filter also features a flat in-band magnitude response and good group delay.

To achieve high rejection ratio at the cutoff frequency as required in Fig. 1(b), the number of order for Butterworth LPF (n_{Bu}) calculated from (1) should be larger than 20 based on the theory analysis in [14], resulting in a very complex, large chip size, high power consumption circuit, and large group delay. n_{Bu} can be expressed by
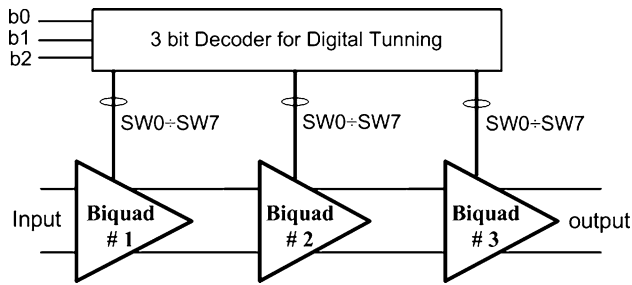
Fig. 2 Block diagram of the 6th order Op-amp RC LPF

$$n_{\text{Bu}} = \frac{\log[(10^{0.1\alpha_{\min}} - 1)/(10^{0.1\alpha_{\max}} - 1)]}{2\log(\omega_s/\omega_p)} \qquad (1)$$

where ω_s and ω_p is the stop-band and pass-band frequency, $\alpha_{\max}$ is the ripple at the pass-band and $\alpha_{\min}$ is the attenuation at the stop-band. Because of that, 6th order LPF topology is chosen as a compromise of those constraints. The whole structure of 6th order LPF is shown in Fig. 2 with three biquad stages. In order to satisfy the sharp rejection ratio and obtain high cutoff frequency, a new technique is proposed which employs the steep slope around the peaking point.

3 Proposed sharp rejection techniques

3.1 Biquad superposition

To obtain high rejection ratio or steep roll-off characteristic, the steep slope due to a high Q transfer function is taken advantage. The three biquads shown in Fig. 2 are designed with different AC characteristics and Q-factors. These biquads transfer functions are superimposed to extend the cutoff frequency and exploit the steep roll-off. Figure 3 demonstrates the proposed technique. Each biquad has the different peaking, which depends on the Q-factor, at different cutoff frequencies. When cascading them, the frequency responses are combined, at the filter cutoff frequency, sharpest slope is obtained while a flat AC response is achieved at other frequencies in the pass-band.

From Fig. 3, biquad 1 has highest Q (≈ 10) peaking at the cutoff frequency (at 264 MHz), leading to a sharp slope. In contrast, Biquad 2 (Q ≈ 0.5) shows a major attenuation at the cutoff frequency to roughly compensate with a relatively high gain peaking in the frequency response of biquad 1. Biquad 3 is needed to smoothly compensate with the combination response of biquad 1 and biquad 2. Therefore, biquad 3 is supposed to have a moderate peaking (Q ≈ 1.6) at a lower frequency (around 150 MHz). The peaking frequency of biquad 3 should be in between the cutoff frequency of biquad 1 and 2. It is chosen based on the relation with the Q-factor values of
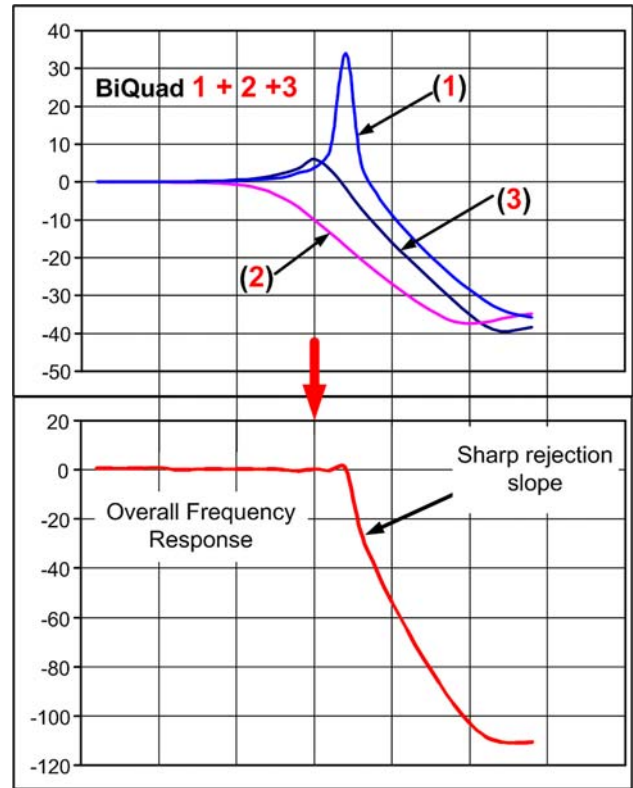
Fig. 3 Combination of three different biquad's AC characteristics

the other two biquads. As a rule of thumb, it is inversely proportional to the Q-factor of biquad 1. From the simulation, the peaking frequency of biquad 3 should be selected to be around 60% of the filter's cutoff frequency. At this frequency, the compensation is easy to be made while reserving the sharp slope characteristic. The role of biquad 3 is to raise the frequency response around these frequencies (150 MHz), which is reduced by biquad 2 and partly contribute further attenuation apposing the peaking of biquad 1 around the cutoff frequency. As a result, when the three biquads' frequency responses are combined, a very sharp rejection is achieved at the cutoff frequency with flat frequency response over the remaining pass-band.

The arrangement of three biquads also affects the noise figure (NF) and linearity performances of the filter depending on the placement of each biquads. The investigation of this effect is in the following.

3.2 Noise and linearity considerations

The three-biquad filter can be generalized as a system of three stages with different gain, Q-factor, and noise figure characteristics.

Thus, the NF can be estimated using Friis' equation [15].

$$NF_{tot} = NF_1 + \frac{NF_2 - 1}{G_1} + \frac{NF_3 - 1}{G_2} \qquad (2)$$

Based on the above equation, the arranging order of three biquads can help reduce the noise figure (NF). The NF is dominated mostly by the first stage, thus, the first stage should have higher gain or high Q for gain peaking. However, it is not intuitive to determine which biquad should stand in the second and third stages in order to achieve the minimum NF. Using the simulator, in Fig. 4, the NF data of all the possible arrangements of the three biquads are provided.

From Fig. 4, the NF performance varies respectively with the biquad arrangements. The worst case is with the biquad combination of 2-3-1. Which agrees with the prediction since the first stage, biquad 2, has the lowest gain. This combination shows an average NF of around 21 dB along the pass-band. The minimum average NF is achieved with the biquad combination of 1-3-2. With this combination, the biquad 1 with the highest gain stands in the first stages followed by the biquad 3 with a moderate gain, and the last stage is the biquad 2 with the lowest gain characteristic. Its average NF is around 13 dB, showing 8 dB of improvement in NF compared with the combination of 2-3-1.

The biquad placements also show an impact on the linearity of the designed filter. Specifically, it is the input voltage which can be handled by the filter or voltage 1 dB compression point (V1 dB). If the first stage has too high gain, the input signal is amplified, thus the filter can easily be saturated. As a rule of thumb, in order to accommodate high input signal voltage, a low gain stage should be placed first. This point seems to be contradicting with the condition for the minimum NF. Therefore, the V1 dB performances of all possible biquad combinations are simulated to find out the optimal arrangement for both NF and V1 dB performance. Figure 5 shows the V1 dB

Fig. 5 1 dB voltage compression point (V1 dB) performance of the LPF for different biquad arrangements

performance of all possible biquad combinations. From Fig. 5, the best V1 dB is obtained with the biquad combination of 2-3-1. From Fig. 4, this combination exhibits the worst NF. It is the trade-off between NF and linearity performances.

Based on Figs. 4 and 5, one can find the optimal combination for a good NF and V1 dB performance is 1-2-3. Thus, the filter will be designed following this biquad combination.

4 LPF designs

4.1 Biquad

A biquad is shown in Fig. 6 equivalent to a 2nd order LPF. It consists of two op-amps and other passive components, R and C. The transfer function of the biquad can be expressed as

$$T(s) = \frac{-1/R_1 R_3 C_1 C_2}{s^2 + (1/R_2 C_2)s + 1/R_2 R_3 C_1 C_2} \qquad (3)$$

From (3), the cutoff frequency (ω_{cutoff}), Q-factor and gain (H) of the biquad are determined by R and C values as

$$\omega_{cutoff} = 1/\sqrt{R_2 R_3 C_1 C_2}, \qquad (4)$$

$$Q = \sqrt{R_4^2 C_2 / R_2 R_3 C_1}, \qquad (5)$$

and $H = R_2/R_1$, respectively. As described above, each biquad has different Q-factor and f_c. Therefore, by changing the values of the passive components, desired AC characteristics are obtained for each biquad. As a guideline for the selection of component values, C_1 and C_2 are chosen equal, so are the value of R_2 and R_3. At a given cutoff frequency, $R_{2,3}$ and $C_{1,2}$ are determined, thus R_4 is

Fig. 4 Noise figure of the LPF for different biquad arrangements
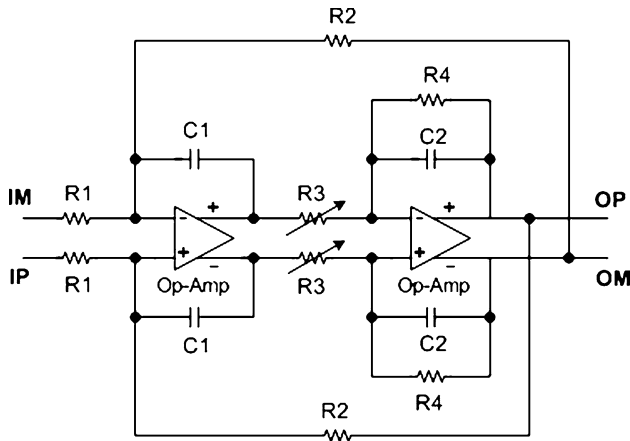
Fig. 6 2nd order biquad structure

varied for obtaining different Q-factor values for each biquad without changing f_c. To change the cutoff frequency, the value of R_3 is varied, which will be discussed in the Section 4.3.

4.2 Op-amp design

Operational amplifier (op-amp) is the core circuit in designing the RC LPF. It will determine the frequency characteristics, linearity and voltage swing of the whole LPF. In order to have high frequency performance, a low-complexity op-amp is adopted in this design, shown in Fig. 7.

The op-amp has two stages, gain stage and output buffer. The NMOS source follower buffer stage has the unity gain and its main function is to maintain the high frequency performance and for the output impedance matching. Degeneration resistor R of the fist stage is used to increase the linearity of the op-amp as well as the overall LPF. R is
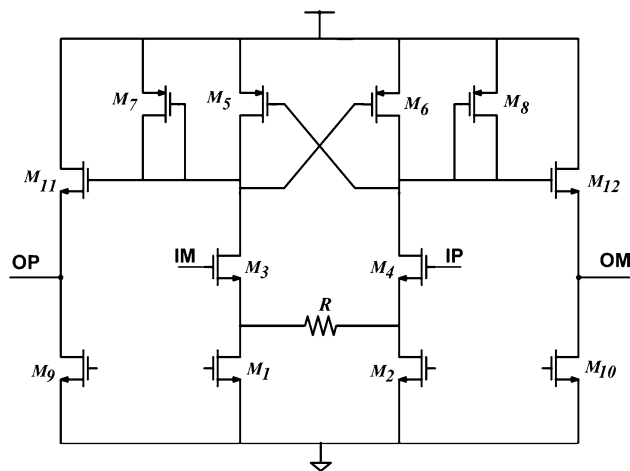
Fig. 7 Op-amp topology

chosen as 40 Ohm to ensure good linearity while maintain high enough DC gain of the Op-amp.

In the first stage, due to the tradeoff between the current consumption and gain, a cross connection at the PMOS load transistors is adopted to ensure high DC gain for a given limited amount of current dissipation. Diode connected in parallel with cross-coupled PMOS transistors ($M_{5,6}$) are used as the load of the op-amp. The gain of the op-amp without cross-coupled PMOS ($M_{5,6}$) is represented by

$$A_V = \frac{g_m \times R_L}{1 + g_m \times R_{degeneration}} \qquad (6)$$

where $R_L = 1/g_{mp}$, g_m and g_{mp} are the transconductance of transistor $M_{3,4}$ and $M_{7,8}$, respectively. With the presence of cross-coupled PMOSs, the total conductance (G_{total}) at the output is reduced [16], leading to the improvement of the gain given in (6) due to the increase of R_L as follows

$$R_L = \frac{1}{G_{total}} = \frac{1}{g_{mp7} - g_{mp6} + g_{ds3} + g_{ds4} + g_{ds5}} \qquad (7)$$

From (7), when $g_{mp7,8}$ and $g_{mp5,6}$ are designed with close values, R_L can be significantly increased and so is the gain.

Another advantage of the op-amp shown in Fig. 7 is self-biasing. No current reference or common mode feedback is required for the load avoiding additional power dissipation. However, the g_m cancellation for gain enhancement only occurs effectively when both output voltages are close to each other. That is the tradeoff of the implemented op-amp for its high DC gain characteristic and simplicity.

The op-amp may experience a slight mismatch and cause positive feedback and instability. To ovoid such issues, the proposed op-amp characteristics are investigated and design guidelines are provided as follows.

The feedback loop gain can be given as in [16] by

$$A_{Loop} = \frac{g_{mp5}}{g_{ds7} + g_{mp7} + g_{ds5} + g_{ds3}} \qquad (8)$$

From (8), A_{loop} must be smaller than unity to avoid the stability problem, which means that $g_{mp5} < g_{ds7} + g_{mp7} + g_{ds5} + g_{ds3}$. Therefore, the rule of thumb for the selection of transistor sizes is $g_{mp5,6} < g_{mp7,8}$.

The op-amp has two poles, the dominant one is at the output node and the other one is at the drain of PMOS load transistors. Those transistor sizes are selected with small channel length to put this pole far away from the dominant one. Thus, the op-amp shows very high frequency characteristic. The simulated gain-bandwidth product of the proposed op-amp is around 2 GHz at the unity gain. The DC gain and phase responses of the op-amp are shown in Fig. 8. Its DC gain is around 47 dB, and the phase margin is 88°, which is good enough to keep the op-amp stable.

Fig. 8 Simulation AC
characteristic of the Op-amp

AC Response

A: (2.04201G 15.095m)   delta: (2.00893M −88.2459)
B: (2.04402G −88.2308)   slope: −43.9267u
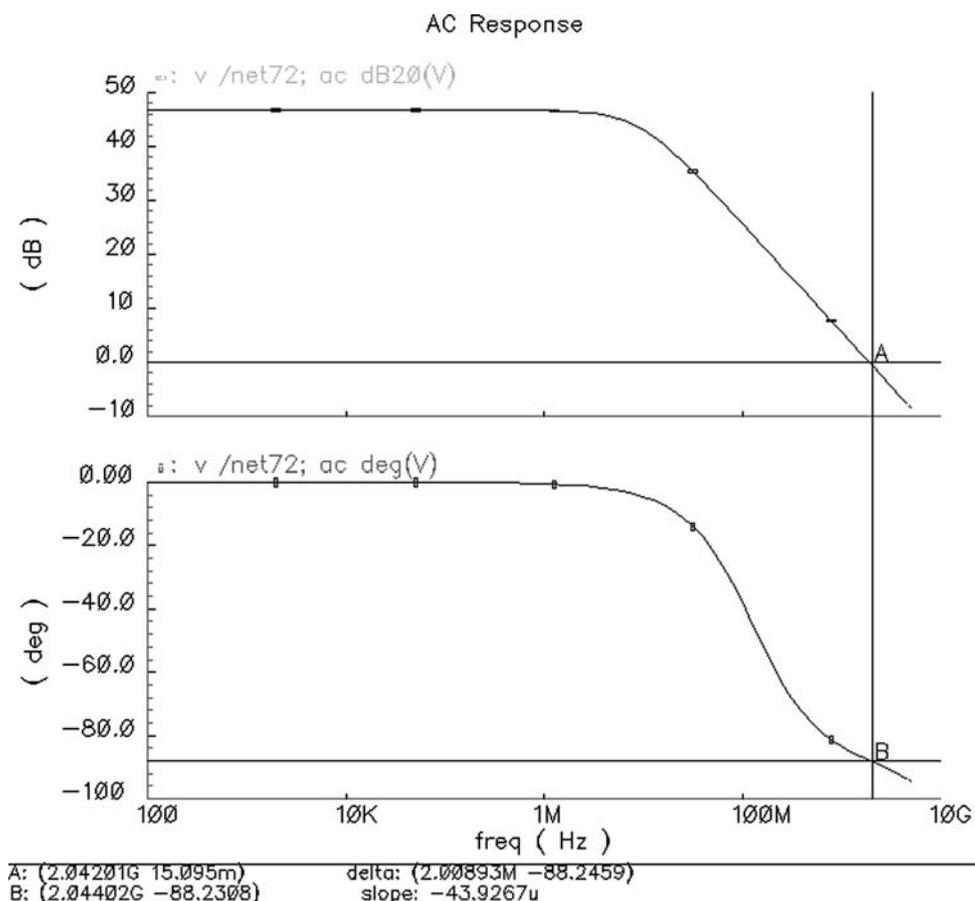
4.3 Tuning circuitry

An important issue in practical continuous time filter
design is the corner frequency variation due to process,
temperature and supply voltage variation.

The cutoff frequency is set by the values of Rs and Cs in
Fig. 6, however, those values can vary as much as 25%. In
order to deal with this practical issue, in this design, a
digital tuning circuit is adopted. From (4), by varying the
value of resistor R_3, the cutoff frequency can be changed.
The capacitor value tuning is not chosen because the value
of capacitor is small and close to the parasitic value and
very sensitive to process variation, thus, the tuning is not
accurate. 3 control bits ($b_{0/2}$) are used at the input resulting
8 frequency tuning steps at the output. An array of 8
resistors with different values from r0 to r7 is implemented
at the position of R_3 in each biquad. The bits ($b_{0/2}$) will
simultaneously control the values of R_3 in these biquads.
The decoder composed of logic components, translates the
3 input control bits into one of 8 outputs for respective
cutoff frequency control. The output of the decoder will
turn on the switch, SW0/SW7, as a result, selecting the
right value of the resistor R_3 corresponding to the input bits
combination for a given cutoff frequency. The digital
tuning block diagram is shown in Fig. 9.

When R_3 is varied for tuning function, the overall
Q-factor of the filter is changed leading to peaking
behavior of the LPF characteristic. In order to keep the
pass-band flat, from (5), R_4 is varied accordingly to keep
Q unchanged at a given cutoff frequency.

5 Experimental results

The UWB LPF is designed using 0.13-μm CMOS tech-
nology with the voltage supply of 1.5 V.

The frequency transfer characteristic of the designed
LPF is shown in Fig. 10. The cutoff frequency at 1 dB is
264 MHz. At 290 MHz the rejection is 12 dBr, and is
about 50 dBr at twice the channel bandwidth, 528 MHz.
The sharp rejection at the cutoff frequency is in agreement
with the prediction. This filter shows very sharp slope over
the range from 264 to 290 MHz, compared to other filters
of the same order by cascading a number of low order filter
stages [17]. Measurement results show 5 MHz shift com-
pared to simulation. This frequency shifting is small
compared to the bandwidth of a UWB channel and toler-
able thanks to the frequency tuning function.

The designed LPF is tunable, nearly 40% around the
cutoff frequency. 3-bit digital control results in 8 frequency
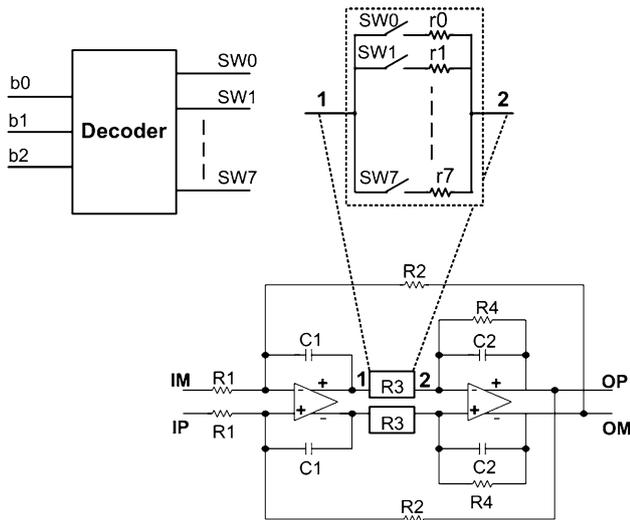
Fig. 9 Digital tuning circuit diagram

tuning steps with a wide tuning range from 190 to 310 MHz. Filter characteristic is quite flat with the ripple varying around 1 dB over the entire tuning range. As can be seen from Fig. 10, at the maximum cutoff frequency, the LPF shows a peaky characteristic with highest ripple of 1.2 dB. As the cutoff frequency decreases, the ripple reduces.

Post-layout simulation shows the group delay value of around 5ns and almost constant along the pass-band, shown in Fig. 11. At the cutoff frequency, the group delay experience a peaking with the value of 9ns due to high Q-factor.

In Fig. 12, two-tone in-band test at 30 MHz and 40 MHz is shown. IM3 is about −44 dB which shows low

3rd order nonlinearity interference on the designed filter. As a result, high linearity performance with 23 dBm of IIP3 and P1 dB is 3 dBm is achieved. The IIP3 and P1 dB measurement results are shown in Fig. 13. Considering the low supply voltage of 1.5 V, the designed filter shows a very good linearity performance.

The measured NF of the UWB LPF is shown in Fig. 14. The estimated averaged NF is around 18 dB over the pass-band with the input referred spectral noise density of about 15.8 nV/$\sqrt{\text{Hz}}$. It increases rapidly in the stop-band due to the sharp decrease in gain of the designed LPF characteristic.
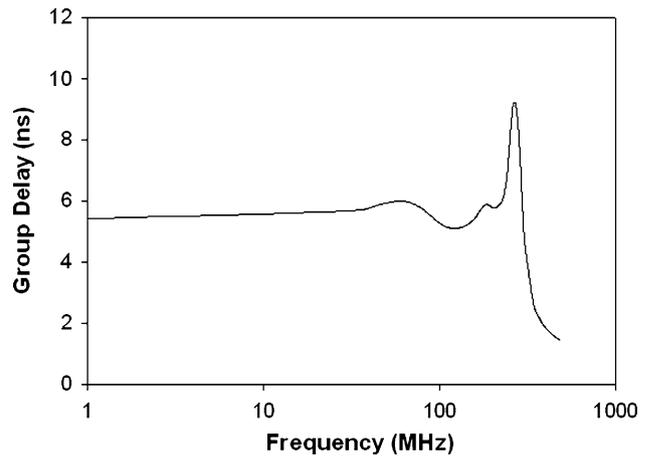
Fig. 11 Post-layout simulation of group delay of the implemented LPF

Fig. 10 Measured tunable transfer function of the designed UWB LPF
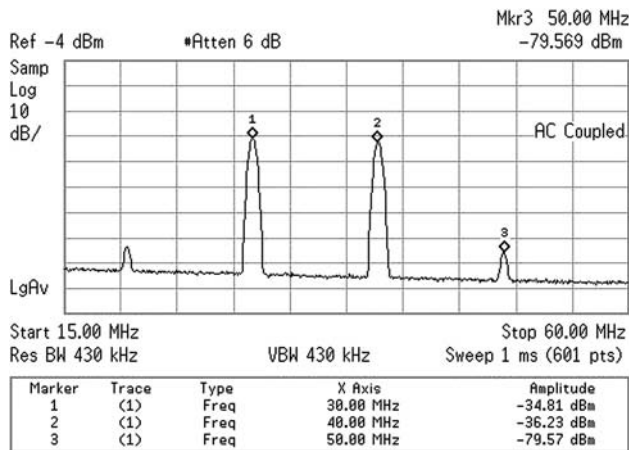
Fig. 12 Two-tone in-band IM3 test at 30 and 40 MHz
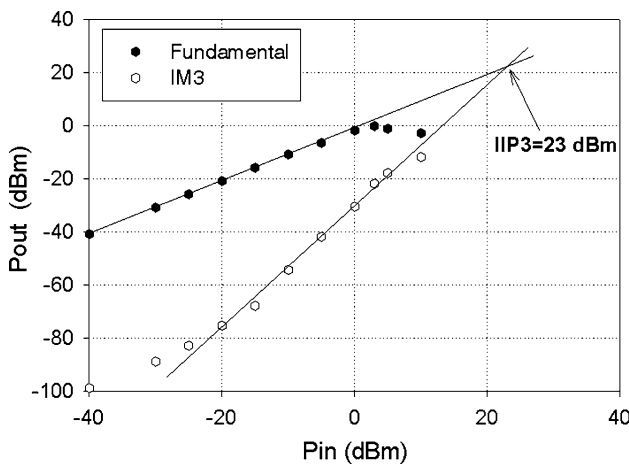
Fig. 13 IIP3 and P1 dB of the designed LPF
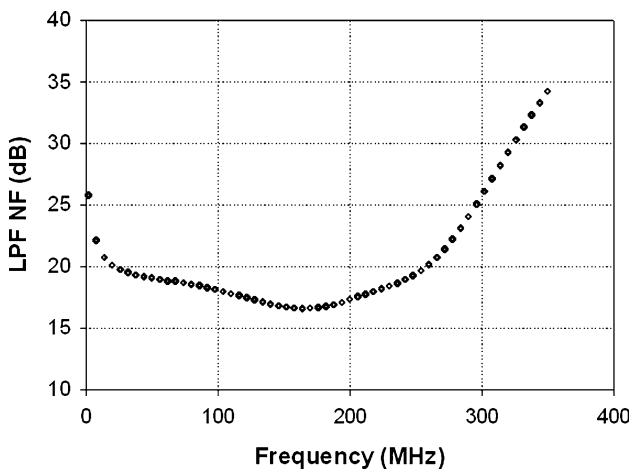
Fig. 14 Measured NF of the designed UWB LPF

The total current consumption of the LPF is 8 mA, or 12 mW. Digital tuning circuit consumes almost no DC current. The LPF performance of this work is summarized

Table 1 UWB LPF performance summary

Parameters	Measurement results
Filter type	6th order RC Butterworth
Cutoff frequency	264 MHz
Rejection	l2 dBr at 290 MHz
	50 dBr at 528 MHz
Tuning range	190 M–310 MHz
V1 dB	300 mVpp
11P3	23 dBm
Group delay	5 ns ± 8%
NF (average)	18 dB
Current consumption/supply voltage	8 mA/1.5 V
Die size	0.25 mm^2
Process	0.13-μm IBM CMOS

in Table 1 and is compared with previously reported works of high frequency LPF designs in Table 2. Based on the defined figure of merit (FOM) in [18, 19], a modified FOM is proposed (9) to provide an accurate comparison of the performance of the designed LPF with previous publications. Since the pole's frequency is proportional to the transconductance which is proportional to the square-root of the bias current, doubling the bandwidth requires 4 times increase of current. Therefore, the square of filter cutoff frequency (f_c) as in [19] and minimum technology size (L) are taken into account for fair comparison in different technology. The proposed FOM is expressed as

$$FOM = \frac{[fc(\text{MHz})]^2 \times L(\mu m) \times \text{SFDR(dB)}}{[P(\text{mW})/N]} \quad (9)$$

where P is the total power consumption, N is the number of poles, and SFDR is the spurious free dynamic range. As can be seen from Table 2, the proposed LPF shows the best performance with the smallest power consumption compared to other state-of-the-art LPFs for wideband applications.

In Fig. 15, the die micrograph is shown with the core size of 400 × 640 μm. All the components are integrated on chip with ESD pads.

6 Conclusion

A wideband, high linearity sharp-rejection op-amp RC LPF for UWB system is proposed and implemented in 0.13-μm CMOS process. The circuit techniques for the bandwidth extension and sharp stop-band characteristic are proposed by superimposing the biquads with different cutoff frequencies and Q-factors. The NF and linearity characteristics related to the biquad arrangements are also analyzed to find the optimal performance. The measurements show 264 MHz of cutoff

Table 2 High frequency LPF performance comparison

Parameters	[6]	[8]	[9]	[10]	[19]	[20]	[21]	This work
Technology (CMOS)	0.l3 μm	0.35 μm	0.35 μm	0.25 μm	0.35 μm	0.18 μm	0.18 μm	0.13 μm
Filter type	G_m-C	Linear phase	Linear phase	Eq.Rip	G_m-C	Op-amp RC	Linear phase	RC Butterworth
Filter order	5	7	4	7	4	5	5	6
Cutoff freq (MHz)	240	200	150	250	550	350	750	264
Supply voltage (V)	1.2	3.3	2.3	2	±1.65	1.8	1.8	1.5
Noise ($nV/\sqrt{Hz}$)	7.7	64.8	1.69 mV$_{rms}$	3	l47 dBm/Hz	24	–	15.8
Input voltage swing (mV)	–	500	200	250	–	500	–	300
SFDR (dB)	–	50	52	65	–	52	58	62
Power consumption (mW)	24	60	90	216	140	25.2	240	12
FOM	–	81.6×10^3	18.2×10^3	32.9×10^3	–	227×10^3	3.16×10^3	280×10^3
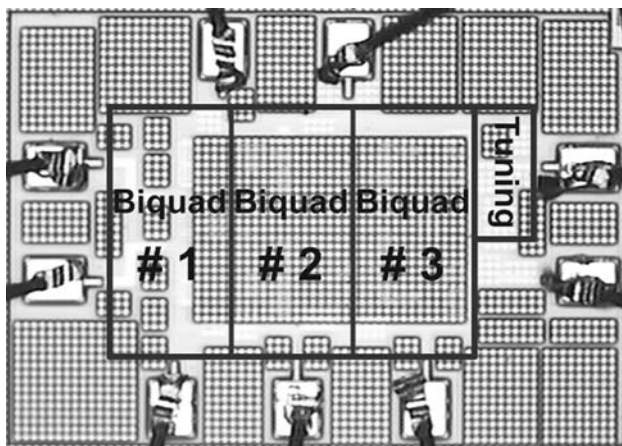
Fig. 15 Die photo of the LPF, 400 × 640 μm

frequency with nearly 40% digital tuning range to deal with process variation. The amount of stop-band rejection is 12 and 50 dBr at 290 and 528 MHz, respectively. The in band ripple is less than 1 dB leading to nearly constant group delay entire the pass-band. In-band two-tone test shows good linearity with 23 dBm of IIP3. The LPF consumes 8 mA from 1.5 V supply and the die size is 400 × 640 μm. The designed filter, compared to other early designs of wideband active-RC LPF, shows very good performance making it suitable for wideband applications like UWB.

References

1. First report and order.revision of part 15 of the commission's rules regarding ultra-wideband transmission systems FCC, 2002, ET Docket 98-153.

2. Batra, A., Balakrishnan, J., Aiello, G. R., Foerster, J. R., & Dabak, A. (2004). Design of a multiband OFDM system for realistic UWB channel environments. *IEEE Transactions on Microwave Theory and Techniques, 52*(9), 2123–2138. doi: 10.1109/TMTT.2004.834184.

3. Valdes-Garcia, A., Mishra, C., Bahmani, F., Silva-Martinez, J., & Sanchez-Sinencio, E. (2007). An 11-Band 3–10 GHz Receiver in SiGe BiCMOS for Multiband OFDM UWB Communication. *IEEE Journal of Solid-State Circuits, 42*(4), 935–948. doi: 10.1109/JSSC.2007.892160.

4. Bergervoet, J., Harish, K., van der Weide, G., Leenaerts, D., van de Beek, R., Waite, H., et al. (2005). An interference robust receive chain for UWB radio in SiGe BiCMOS. In: *ISSCC Digest of Technical Papers*, (pp. 214–215).

5. Iida, S., Tanaka, K., Suzuki, H., Yoshikawa, N., Shoji, N., Griffiths, B., et al. (2005). A 3.1 to 5 GHz CMOS DSSS UWB transceiver for WPANs In: *ISSCC Digest of Technical Papers*, (pp. 214–215).

6. Saari, V. Mikko Kaltiokallio, Saska Lindfors, Jussi Ryynänen, & Kari Halonen. (2007). A 1.2-V 240-MHz CMOS continuous-time low-pass filter for a UWB radio receiver. *ISSCC Digest of Technical Papers*.

7. Tsividis, Y. P. (1994). Integrated continuous-time filter design-an overview. *IEEE Journal of Solid-State Circuits, 29*(3), 166–176. doi:10.1109/4.278337.

8. Silva-Martinez, J., Adut, J., Rocha-Perez, M., Robinson, M., & Rokhsaz, S. (2003). A 60-mW 200-MHz continuous-time seventh-order linear phase filter with on-chip automatic tuning system. *IEEE Journal of Solid-State Circuits, 38*(2), 216–225. doi:10.1109/JSSC.2002.807402.

9. Chen, M., Silva-Martinez, J., Roskhsaz, S., & Robinson, M. (2003). A 2 Vpp, 80-200-MHz fourth-order continuous-time linear-phase filter with automatic frequency tuning. *IEEE Journal of Solid-State Circuits, 38*(10), 1745–1749. doi:10.1109/JSSC.2003.817595.

10. Masood-ul-Hasan, & Yichuang Sun. (23–26 May 2005). 2 V 0.25 μm CMOS 250 MHz fully-differential seventh-order equiripple linear phase LF filter. In: *IEEE International Symposium on Circuits and Systems (ISCAS)*, (pp. 5958–5961).

11. Bollati, G., Marchese, S., Demicheli, M., & Castello, R. (2001). An eighth-order CMOS low pass filter with 30–120 MHz tuning range and programmable boost. *IEEE Journal of Solid-State Circuits, 36*(7), 1056–1066. doi:10.1109/4.933461.

12. D'Amico, S., De Matteis, M., & Baschirotto, A. (2008). A 6th-order 100 μA 280 MHz source-follower-based single-loop continuous-time filter. In: *ISSCC Digest of Technical Papers*, (pp. 72–73).

13. Roovers, R., Leenaerts, D. M. W., Bergervoet, J., Harish, K. S., van de Beek, R. C. H., van der Weide, G., et al. (2005). An

interference-robust receiver for ultra-wideband radio in SiGe BiCMOS technology. *IEEE Journal of Solid-State Circuits, 40*(12), 2563–2572. doi:10.1109/JSSC.2005.857431.

14. Rolf, S., & Van Valkenburg, E. M. (2001). *Design of analog filter*. New York: Oxford Press.

15. Friis, H. T. (Jul. 194). Noise Figure of Radio Receivers. *Proc. IRE*, Vol. 32, (pp. 419–422).

16. D'Amico, S., Ryckaert, J., & Baschirotto, A. (Sept.). A up-to-1 GHz low-power baseband chain for UWB receivers. In: *IEEE European Solid-State Circuits Conference* (*ESSCIRC*), (pp. 263–266).

17. Thirugnanam, R. Dong Sam Ha, Bong Hyuk Park, S., & Choi, S. (May 2006). Design of a tunable fully differential GHz range Gm-C lowpass filter in 0.18 /spl mu/ m CMOS for DS-CDMA UWB transceivers. *IEEE International Symposium on Circuits and Systems* (*ISCAS*).

18. Yoshizawa, A., & Tsividis, Y. P. (2002). Anti-blocker design techniques for MOSFET-C filters for direct conversion receivers. *IEEE Journal of Solid-State Circuits, 37*(3), 357–364. doi:10.1109/4.987088.

19. Pandey, P., Silva-Martinez, J., & Liu, X. (2006). A CMOS 140-mW fourth-order continuous-time low-pass filter stabilized with a class ab common-mode feedback operating at 550 MHz. *IEEE Transactions on Circuits Systems-Part I, 53*(4), 811–820. April.

20. Harrison, J., & Weste, N. (2002). 350 MHz opamp-RC filter in 0.18 um CMOS. *Electronics Letters, 38*(6), 259–260. doi:10.1049/el:20020205.

21. Zhu, X., Sun, Y., & Moritz, J. (May 2008). A CMOS 750 MHz fifth-order continuous-time linear phase lowpass filter with gain boost *IEEE International Symposium on Circuits and Systems* (*ISCAS*), (pp. 900–903).

Ronan Farrell is from Clondalkin, Dublin, Ireland. He graduated from University College Dublin in 1993 with a B.E. and proceeded to work with ICI/Zeneca Chemicals for the next 2 years in Louisiana, USA, and on various sites in Yorkshire, England. In 1995 he returned to University College Dublin to start on a Masters on Sigma-Delta Modulators, sponsored by Analog Devices. This developed into a Ph.D., which he received in 1998. After receiving his Ph.D. he joined Silicon Systems Limited (SSL) which was to become Parthus Technologies after going public. He worked within the mixed signal group designing custom silicon chips, ranging from low frequency, low power, applications to 2.4 GHz phase-lock loops. His areas of expertise are in system modelling and development, digital and analog design at low and medium frequencies, and in particular data converters utilising oversampling techniques. He left Parthus Technologies in 2001 and took an academic position with the National University of Ireland, Maynooth. Currently he is a lecturer in the Department of Electronic Engineering at NUI, Maynooth. His courses currently include Analog Electronics (GE204) and Solid State Electronics (GE201).

Anh Tuan Phan was born in Hanoi, Vietnam in 1979. He received the B.S. degree (5-year degree) in Electronics and Telecommunications from Hanoi University of Technology, Vietnam, in 2002, and the M.Sc. and Ph.D degrees in Electrical Engineering from Information and Communications University, Daejeon, Korea, in August 2004 and February 2008 respectively. He was with Electronic and Telecommunication Research Institute (ETRI), Korea from April 2007 to October 2007 as an intern for the development of the Pulse-Based UWB Transceiver for WPAN. He is now with the Institute of Microelectronics and Wireless Systems, National University of Ireland, Maynooth, Ireland, as a Post Doctoral Researcher. His current research interests are CMOS RFIC design, UWB radio transceiver design, Reconfigurable radio, and low power low cost circuit solutions.

Sang-Gug Lee was born in Gyungnam, Korea in 1958. He received the B.S. degree in Electronic Engineering from the Gyungbook National University, Korea, in 1981, and the M.S. and Ph.D. degrees in Electrical Engineering from the University of Florida, Gainesville, in 1989 and 1992, respectively. In 1992, he joined Harris Semiconductor, Melbourne, Florida, USA, where he was engaged in silicon-based RF IC designs. From 1995 to 1998, he was with Handong University, Pohang, Korea, as an assistant professor in the school of Computer and Electrical Engineering. Since 1998, he is with Information and Communications University, Daejeon, Korea, where he is now a professor. His research interests include the silicon technology-based (BJT, BiCMOS, CMOS, and SiGe BICMOS) RF IC designs such as LNA, mixer, oscillator, power amp, etc. He is also active in the high-speed IC designs for the optical communication such as the TIA, driver amp, limiting amp, CDR, mux/demux, etc.